

Study of nucleic acid–gold nanorod interactions and detecting nucleic acid hybridization using gold nanorod solutions in the presence of sodium citrate^{a)}

Roejarek Kanjanawarut and Xiaodi Su^{b)}

*Institute of Materials Research and Engineering, Agency for Science, Technology and Research (A*STAR),
3 Research Link, Singapore 117602, Singapore*

(Received 23 August 2010; accepted 15 September 2010; published 14 December 2010)

In this study, the authors report that sodium citrate can aggregate hexadecyl-trimethyl-ammonium ion⁺-coated gold nanorods (AuNRs), and nucleic acids of different charge and structure properties, i.e., single-stranded DNA (ssDNA), double-stranded DNA (dsDNA), single-stranded peptide nucleic acid (PNA), and PNA-DNA complex, can bind to the AuNRs and therefore retard the sodium citrate-induced aggregation to different extents. The discovery that hybridized dsDNA (and the PNA-DNA complex) has a more pronounced protection effect than ssDNA (and PNA) allows the authors to develop a homogeneous phase AuNRs-based UV-visible (UV-vis) spectral assay for detecting specific sequences of oligonucleotides (20 mer) with a single-base-mismatch selectivity and a limit of detection of 5 nM. This assay involves no tedious bioconjugation and on-particle hybridization. The simple “set and test” format allows for a highly efficient hybridization in a homogeneous phase and a rapid display of the results in less than a minute. By measuring the degree of reduction in AuNR aggregation in the presence of different nucleic acid samples, one can assess how different nucleic acids interact with the AuNRs to complement the knowledge of spherical gold nanoparticles. Besides UV-vis characterization, transmission electron microscopy and zeta potential measurements were conducted to provide visual evidence of the particle aggregation and to support the discussion of the assay principle. © 2010 American Vacuum Society. [DOI: 10.1116/1.3496962]

I. INTRODUCTION

Noble metal nanoparticles (mNPs) have unique optical properties arising from their ability to support a localized surface plasmon resonance (LSPR).^{1,2} The particle size-determined, spacing-determined, and aggregation-determined LSPR properties have been extensively exploited for developing colorimetric bioassays.^{3–5} Biomolecular binding events and biological processes can be detected because they can modulate the mNPs' dispersion and aggregation status. Changing of the interparticle distance will change the plasmonic coupling properties that are measurable by a distinct solution color change and a LSPR spectrum shift.⁵

Spherical mNPs (gold, silver, and SiO₂ at Au core-shell, etc.) have been the primary choice of colorimetric probes. Numerous assays have been developed for a wide range of analytes (e.g., DNA, protein, metal ions, enzyme, and small molecular drugs).⁵ These assays exploit interparticle crosslinking and noncrosslinking aggregation mechanisms that usually involve receptor-conjugated mNPs and unmodified mNPs, respectively. Compared to the extensive research with the spherical nanoparticles, the use of nonspherical particles with anisotropic configuration to construct plasmon

coupling-based colorimetric assays has been less well demonstrated, except for a few examples using gold nanorods (AuNRs).^{6–13}

AuNRs exhibit two plasmon resonance bands, i.e., transverse and longitudinal bands, corresponding to electron oscillation along the short axis and the long axis, respectively. The longitudinal peaks can be shifted to a near infrared region and are highly sensitive to changes in local environment and interparticle spacing.¹⁴ Similar to the design of the spherical mNP-based assay, nanorods are usually functionalized with specific receptors (e.g., oligonucleotides,^{6,7} antibody,⁸ crown ethers,⁹ biotin-BSA,¹⁰ and amino acids¹¹). On-particle analyte binding provides aggregation forces to induce color or spectral changes. The distinct features in plasmon spectra associated with nanorods assembled through side-by-side^{6,9} or end-by-end arrangement^{7,9,11,15–17} provide additional measures for surfaces on which the receptors are attached and for the binding nature between receptors and analytes (e.g., binding stoichiometry of metal ions with crown ethers⁹).

AuNRs are usually synthesized in micellar solutions of hexadecyltrimethylammonium bromide [CTA⁺Br⁻ (CTAB)].¹⁴ The resulting AuNRs are coated with a CTA⁺ bilayer, which provides sufficient charge repulsion and steric force to ensure that the nanorods are highly dispersed. Besides the use of receptor-conjugated AuNRs, colorimetric assays have also been developed employing CTA⁺-AuNRs without conjugation of receptors. In an example for detecting DNA hybridization,¹² AuNRs are aggregated in a side-by-side manner through electrostatic attraction between nega-

^{a)}This article is part of an In Focus section on Biointerface Science in Singapore, sponsored by Bruker Optik Southeast Asia, IMRE, the Provost's Office and School of Materials Science and Engineering of Nanyang Technological University, and Analytical Technologies Pte. Ltd.

^{b)}Author to whom correspondence should be addressed; electronic mail: xd-su@imre.a-star.edu.sg

TABLE I. Oligonucleotide sequences.

Oligonucleotides	Sequences	
PNA probe	N'-TTGCACTGTCCTCTTGA-C'	
ssDNA probe	5'-TTGCACTGTACTCCTCTTGA-3'	
Target DNA	Fully complementary (fc)	5'-TCAAGAGGAGTACAGTACAA-3'
	Single base mismatch (m1)	5'-TCAAGAGGAGAACAGTACAA-3'
	Noncomplementary (nc)	5'-CTTACATAGGTAGCACCAACAC-3'

tively charged double-stranded DNA (dsDNA) and positively charged AuNRs.¹⁸ In the example for detecting metal ions (Fe^{2+}),¹³ AuNRs are aggregated through a controlled removal of stabilization forces by negatively charged poly (sodium 4-styrenesulfonate) (PSS).

In this contribution, we develop a UV-visible (UV-vis) spectral assay to detect nucleic acid hybridization using CTA⁺-coated AuNRs through a controlled removal of the stabilization force. Particularly, we use an anionic substance (i.e., sodium citrate) to aggregate the particles in the presence of a single-stranded DNA [or peptide nucleic acid (PNA)] probe before and after its hybridization with its target DNA. We found that the ssDNA (or PNA) probe and the hybridized double-stranded dsDNA (or PNA-DNA complexes) can coat on nanorods and retard the sodium citrate-induced aggregation. More importantly, the effects are more pronounced with dsDNA (PNA-DNA complexes) than PNA probes. We have exploited this phenomenon for DNA detection with single-base-mismatch selectivity. The validity of our current assay is affirmed by the facts that negatively charged substances (e.g., PSS,¹³ sodium citrate,^{19,20} and tris anions²¹) can aggregate the CTA⁺-AuNRs, and the inhibition of these coagulation effects can be used to design colorimetric assays (for Fe^{2+} in the case of PSS as being a coagulant¹³). This current assay involves no tedious probe-AuNRs conjugation and no on-particle hybridization, which is often slow in colorimetric response (0.10 min to hours^{6,21}). The limit of detection (LOD) of this assay is lower than that constructed using spherical gold nanoparticles (AuNPs) with a similar sensing principle (controlled removal of stabilization forces).^{22,23} Besides constructing assays for detecting specific DNA sequences, the second thrust of this study is to understand how different nucleic acids interact with AuNRs. Using AuNRs' aggregation as a measure with the assistance of zeta potential measurements, we have compared the adsorption behaviors of ssDNA, dsDNA, PNA, and PNA-DNA complexes on AuNRs, aiming to complement the knowledge for citrate ion-protected gold nanospheres.^{22–24}

II. MATERIALS AND METHODS

A. Reagents

Supernatant of gold nanorods (de-ionized water with <0.1% ascorbic acid and <0.1% CTAB surfactant capping agent) with an aspect ratio of 3 (25 nm width and 73 nm length) and 3.5 (25 nm width and 86 nm length) were purchased from NanopartzTM Inc. (Loveland, CO). The triso-

dium citrate dihydrate (99.9%) was obtained from Aldrich. A 20 mer single-stranded DNA probe (5'-TTGCACTGTACTCCTCTTGA-3') and their target DNA (fully complementary, noncomplementary, and single-base-mismatch targets) were purchased from Research Biolabs Pte. Ltd. (Singapore). A 20 mer PNA probe of the same sequence was synthesized by the Eurogentec S.A. Leige (Belgium) (see Table I).

B. Apparatus and characterization

The absorption spectra were measured using a TECAN infinite M200 spectrophotometer (Tecan Trading AG, Switzerland) from 96 well microplates. Zeta potential measurements were carried out using a ZETA PLUS zeta potential analyzer (Brookhaven Instruments). Transmission electron microscopy (TEM) images were obtained with a JEOL JEM-2100 TEM operating at 200 kV.

C. Assay procedure

Ninety-six well microplates were used as reaction carriers, and 150 μl of AuNR solutions was used as working volumes. Sodium citrate-induced particle aggregation was detected by an immediate scan of the UV-vis spectra from 400 to 900 nm wavelengths upon addition of sodium citrate (final concentrations of 0.2–1 mM). The detection of specific DNA was performed first by annealing DNA (or PNA) probe (40 μM) with a target DNA at 1:1 molar ratio or varied target/probe ratios (0.01, 0.02, 0.05, 0.1, and 0.5) in a 10 mM phosphate buffer (pH 7.2) containing 100 mM NaCl and 0.1 mM EDTA for 30 min, second by adding the annealing mixture (3.75 μl) into 150 μl of AuNRs, third by adding sodium citrate into the mixture (final concentration 0.5 or 1 mM), and thereafter recording the UV-vis spectra immediately.

III. RESULTS AND DISCUSSION

A. Sodium citrate-induced AuNRs aggregation

Using AuNRs of different aspect ratios (3.0 and 3.5), we have demonstrated that citrate ions can aggregate the particles (Fig. 1, route A) to different degrees, depending on the concentration. Figure 2 shows a representative result for the AR 3.0 nanorods. When sodium citrate is higher than 0.4 mM, the nanorods start to aggregate, characterized as gradual changes of their UV-vis extinction spectra. Particularly, the transverse peak shifts to longer wavelengths ($\Delta\lambda$ up to 30 nm

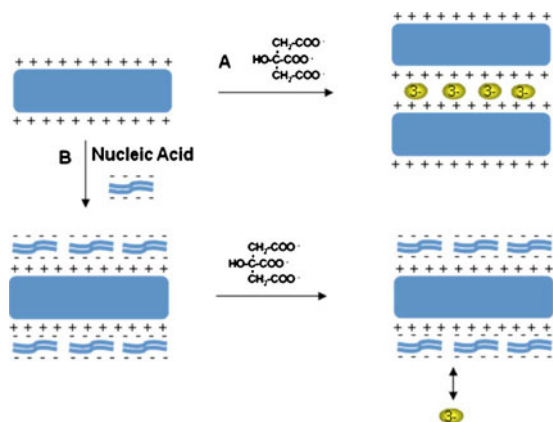


FIG. 1. (Color online) Schematic illustration of the mechanism.

at the highest sodium citrate concentration 1 mM tested) and the longitudinal peak intensity drop (the inset of Fig. 2 shows the average of three repeated experiments) accompanied with slight blueshifts of the peak wavelength (5–10 nm). The redshift of the transverse peak and the blueshift of the longitudinal peak are typical signatures of a side-by-side arrangement of the nanorods in random aggregates.^{19,21} Jain *et al.* observed a similar aggregation profile for CTA⁺-coated AuNRs synthesized in their laboratory.²⁰ They proposed that the particle aggregation is a result of the electrostatic attraction between the positively charged nanorods surface and the negatively charged carboxylate ends of the citrate ions. The adsorbed citrate anions may either bridge between nanorods, or lead to the formation of local negatively charged regions on the nanorod that are electrostatically attracted to cationic regions on adjacent nanorods, or simply neutralize the electrostatic repulsion between the nanorods. We have conducted zeta potential experiments for our AuNRs solutions (AR 3.0) before and after the addition of 1 mM sodium citrate. A drastic reduction of positive charge from $+59.4 \pm 4.8$ (pure AuNRs solution) to $+15.7 \pm 2.1$ (sodium citrate added) was

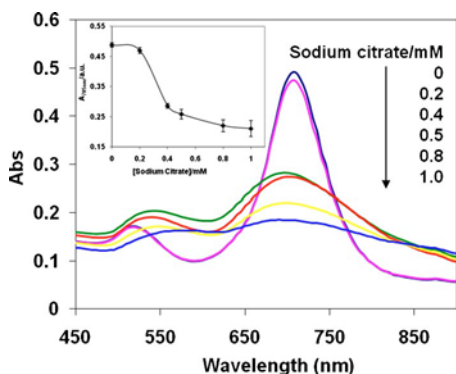


FIG. 2. (Color online) UV-vis extinction spectra of AuNRs (AR 3.0, 218 pM) with the addition of sodium citrate at concentrations of 0, 0.2, 0.4, 0.5, and 1 mM. All spectra were scanned immediately after the addition of sodium citrate. The inset shows the average longitudinal peak intensity ($n = 3$) at a different sodium citrate concentration.

observed, which supports the argument that charge neutralization may be dominantly responsible for the particle aggregation.

B. Oligonucleotides retard the aggregation in a concentration and structure dependent manner

In the following experiments involving oligonucleotides, we found that adding ssDNA (20 mer in this case) and its corresponding dsDNA (ssDNA annealed with its complementary target) (route B in Fig. 1) into AuNRs solutions can retard the sodium citrate-induced aggregation in a DNA concentration and structure dependent manner (Fig. 3). The higher the DNA concentration, the better the protection observed for both dsDNA and ssDNA. More importantly, the effect of dsDNA is more pronounced than ssDNA at a given concentration. The reduced aggregation is detected as smaller redshifts of the transverse peak and less decrease in the longitudinal peak intensity. From Fig. 3(c), a summary of DNA concentration dependent protection effect measured as intensity drop at the longitudinal wavelength (the less intensity drop, the better protection), one can clearly see that dsDNA's protection is better than that of ssDNA at the same concentration and even at a doubled concentration. This means that it is the unique structure of dsDNA attributable to the better protection, but not the total concentration (in dsDNA the total concentration of the DNA strands is about twice that of the ssDNA of same molar concentration). TEM images taken for AuNRs samples containing ssDNA, dsDNA (1 μ M), and 1 mM sodium citrate (Fig. 4) confirm the differential protection effects; i.e., the dsDNA-containing AuNRs remain well dispersed, whereas ssDNA-containing ones underwent a certain degree of aggregation, but being less intensive than those without DNA. We have inferred that it is the adsorption of negatively charged DNA to CTA⁺-coated AuNRs (through electrostatic attraction^{12,18}) that provides charge repulsion and a steric barrier to prevent the citrate anions from coming closer to neutralize the surface charges. We have further speculated that the differential ability of dsDNA and ssDNA to retard the aggregation is due to their distinct charge and structure properties.

To prove that negatively charged ssDNA and dsDNA can bind to CTA⁺-coated AuNRs, we measured the zeta potential of the AuNR solutions (AR 3.5) mixed with DNA. The charge density of CTA⁺-coated AuNRs (zeta potential $+59.4 \pm 4.8$ mV) indeed reduced upon incubation with ssDNA ($+53.3 \pm 1.8$ mV) and dsDNA ($+49.1 \pm 1.6$ mV). The larger degree of reduction with dsDNA coating (17.3%) than ssDNA (10.3%) indicates that the dsDNA coating contributes more negative charges to neutralize the positive charges, which can be accountable for a stronger repulsion to citrate ions and thus a larger degree of protection. The nearly doubled reduction of the positive charge caused by dsDNA relative to the ssDNA seems to suggest that the coating density (the number of DNA molecules per rod) is similar, considering that one dsDNA molecule carries two times negative charges as one ssDNA. In other words, the dsDNA and ssDNA bind comparably well to CTA⁺-coated AuNRs. This is

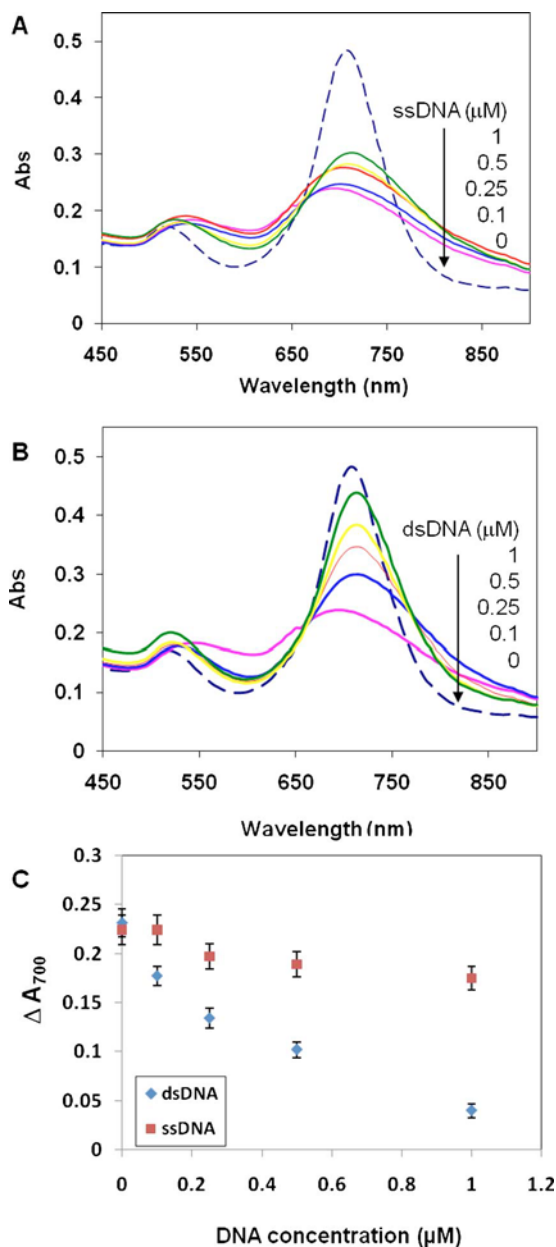


FIG. 3. (Color online) UV-vis extinction spectra of AuNRs solutions (AR 3.0) (dashed lines) and those with the addition of 0.5 mM sodium citrate in the presence of (a) 0–1 μM of ssDNA probe and (b) 0–1 μM dsDNA (the ssDNA probe annealed with its fully complementary target DNA). All spectra were scanned immediately after addition of sodium citrate. Panel (c) shows a summary of DNA concentration dependent protection effect, measured as the drop of intensity at the longitudinal peak wavelength.

unlike the case for citrate anion-stabilized spherical AuNPs, where dsDNA molecules, due to the exposure of negatively charged phosphate backbone, exhibit a much lower affinity than ssDNA that exposes nucleosides to facilitate the coordination interaction with gold.²⁴ In the case of gold nanorods, the “thicker” CTA⁺ bilayer (relative to the citrate anion layer on spherical AuNPs) would not expose sufficient gold surface for coordination binding; as such, the binding of DNA is dominated by electrostatic attraction that makes the double helix structure of dsDNA a favorable geometry.

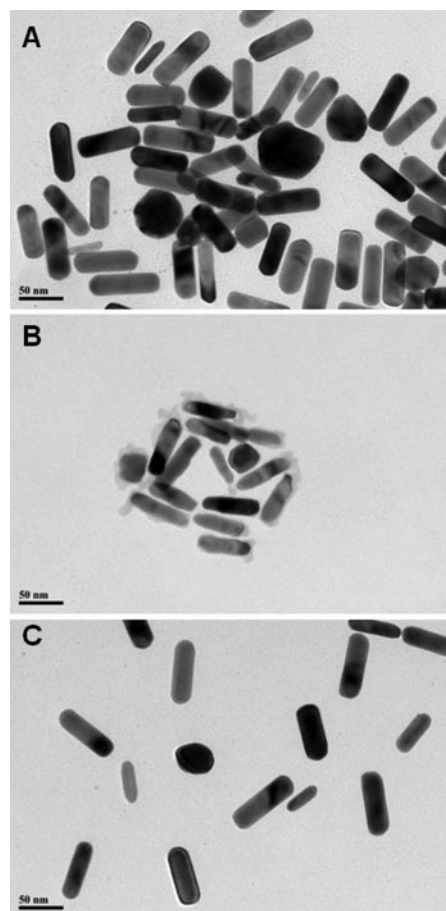


FIG. 4. TEM images of AuNRs (AR 3.0) exposed to 1 mM sodium citrate in the (a) absence of DNA and (b) presence of ssDNA (0.5 μM) and (c) dsDNA (0.5 μM).

It is worth mentioning that the coating of dsDNA and ssDNA (the highest concentration tested of 1 μM) on nanorods did not induce significant changes in the suspension status of the nanorods (in the absence of sodium citrate), as can be seen from their UV-vis spectra (see Ref. 25, Fig. S1). This shows that the remaining positive charges on nanorods with both dsDNA or ssDNA coatings are sufficient to disperse the particles. The addition of sodium citrate is essential to differentiate the presence of dsDNA and ssDNA.

C. Detection of specific DNA sequences using single-stranded DNA probe

The above characteristic, i.e., dsDNA, can retard sodium citrate-induced AuNR aggregation to a larger extent than ssDNA, forms the basis for the design of DNA hybridization assay. In the next experiments, using the 20 mer ssDNA as a sensing probe, we demonstrate that DNA targets containing fully complementary, single-base-mismatch, or partially matched sequences can be differentiated, and the fully complementary DNA can be detected with a LOD of 5 nM.

Figure 5 shows the differential UV-vis adsorption spectra of AuNRs recorded in sodium citrate (0.5 mM) in the presence of the ssDNA probe and its annealing mixtures with either fully complementary (fc), single-base-mismatch (m1),

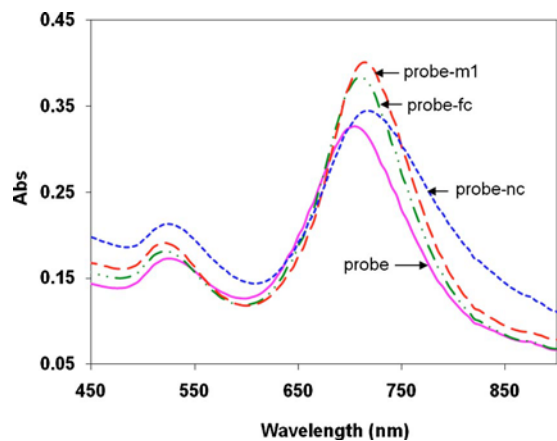


FIG. 5. (Color online) UV-vis extinction spectra of AuNRs solutions (AR 3.0) upon addition of sodium citrate (0.5 mM) in the presence of DNA-DNA complexes with fc, nc, and m1. DNA concentration is 1 μM . All spectra were scanned immediately after the addition of sodium citrate.

or noncomplementary (nc) targets. It is very obvious that the solutions containing these three probe-target mixtures have remarkably different UV-vis spectra, with reference to that containing ssDNA probe without annealing treatment. For the fc and m1 targets, the much higher intensity of the longitudinal peak evidences that the particles remain stable, which can be attributed to the formation of DNA duplexes in the annealing mixtures that protect the particles from aggregation. The shift of the spectrum to the longer wavelength for the m1 target relative to that for fc target indicates a slightly more aggressive aggregation of the nanorods when exposed to the probe-m1 target mixture due presumably to the lower affinity between the probe and the target, and therefore less amount of DNA duplex formed to protect the particles. For the nc target-probe mixture-containing solution, we observed a larger degree of aggregation relative to the fc and m1 targets, evidencing the absence of stable DNA duplex due to the unmatched sequence. On the other hand, the nc target-probe mixture seems to have modulated the particles' behavior differently from the ssDNA without an annealing treatment (a 15 nm difference in their peak wavelength and slightly higher peak intensity in nc target-probe mixture). We analyzed the sequences of the probe and the nc target using a pairwise sequence alignment tool and found that nine bases from the probe and ten bases from the nc target are complementary with each other, which may cause the nc target to bind to the probe with two mismatches and one gap.²⁵ It is then speculated that some partially annealed probe-nc target complexes are present in solution to be responsible for the higher peak intensity (higher AuNRs stability). The possibility of the nc target and the probe sequence to form partially bound duplex is affirmed with the peptide nucleic acid probe in Sec. III D.

To determine the LOD for the fully complementary target, the target DNA was mixed with the ssDNA probe at molar ratio of 0 to 0.5 to attempt the hybridization. After that, they were added into the AuNRs solutions. Figure 6 shows the aggregation profiles of AuNRs (AR 3.5) induced by sodium

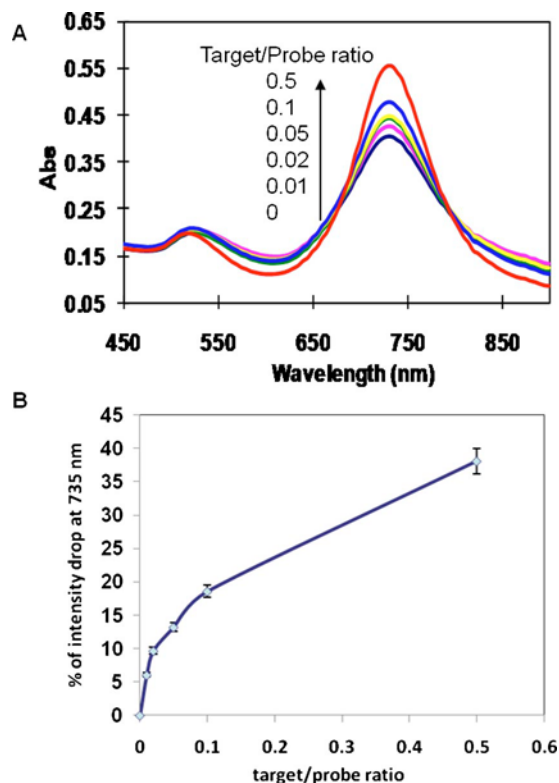


FIG. 6. (Color online) (a) UV-vis extinction spectra of AuNRs (AR 3.5) solutions upon addition of sodium citrate in the presence of DNA probe-target mixtures at target/probe ratio of 0–0.5. All spectra were scanned immediately after addition of sodium citrate. (b) A summary of the relationship between target/probe ratio and percentage drop of longitudinal peak intensity. The ssDNA probe concentration is fixed at 0.5 μM . Sodium citrate concentration is 0.5 mM.

citrate of 0.5 mM in the presence of the probe-target mixtures and the target/probe ratio-determined longitudinal peak intensity changes. At a target/probe ratio of 0.01 (target concentration of 5 nM), the difference in UV-vis spectra is still clearly detectable. The intensity of the longitudinal peak is 6% higher than that of ssDNA alone (target/probe ratio of 0). This increment is more than three times of the relative standard deviation (1.5%) of the average peak intensity of a multiple scan of the AuNRs solutions with ssDNA and sodium citrate (see Ref. 25, Fig. S3). This detection limit (5 nM) is comparable with that of the AuNRs-based crosslinking assays¹² and ten times lower than that using unmodified AuNPs and nonscroslinking mechanism.^{23,24,26}

D. Detection of specific DNA sequences using PNA probe

PNA is a DNA analog in which the entire sugar-phosphate backbone is replaced by a charge neutral polyamide backbone. The distinct backbone properties of PNA (composition and charge) relative to DNA have been exploited to design spherical gold and silver NP-based DNA colorimetric assays in our group.^{22,23} In those studies, we investigated the distinct binding behaviors of ssDNA, PNA, dsDNA, and PNA-DNA complexes to spherical mNPs. In this current study, using sodium citrate-induced AuNR aggregation as a mea-

sure, with the assistance of zeta potential measurement, we for the first time investigated the binding behavior of PNA and PNA-DNA complexes to CTA⁺-coated AuNRs. We have also compared the ability of PNA and PNA-DNA complexes to retard sodium citrate-induced aggregation, aiming to demonstrate the possibility using PNA as a sensing probe for detecting specific DNA sequences.

First of all, we measured the zeta potential of the AuNRs solutions mixed with a 20 mer PNA probe. We found that the positive charge density of the nanorods increased remarkably from $+59.4 \pm 4.8$ mV (before incubation with PNA) to $+77.2 \pm 3.1$ mV (after incubation with PNA). Since one PNA molecule carries one positive charge at the *N*-terminal at neutral *pH*,²⁴ the increase in the positive charge strongly evidenced that PNA molecules bind to the nanorods effectively. Unlike DNA that can bind to AuNRs by electrostatic attractions, PNA may bind to CTA⁺-AuNRs by hydrophobic interactions between the peptide backbone and the alkyl chains of the CTA⁺ bilayer.²⁷ Also, the exposed gold surface at the tips of AuNRs (CTA⁺ bilayer density is lower at tips¹¹) may facilitate the binding through coordination chemistry between gold, the nucleic bases, and the peptide backbone.²⁸

In order to assess the possibility of using PNA as a probe to detect specific DNA, we next tested the sodium citrate-induced AuNRs aggregation in the presence of PNA probe and its annealing mixtures with fc, m1, and nc targets. We have made a few observations from their UV-vis extinction spectra (Fig. 7). First of all, PNA can retard the aggregation, but to a much smaller extent than PNA-DNA complexes. This ensures the idea of using PNA as a sensing probe to detect specific DNA sequences under the proposed assay arrangement. Second, PNA-DNA annealing mixtures with different sequences show differential protection effects, with an order of $fc > m1 > nc$, as shown by their ascendant longitudinal wavelength shift of 5, 10, and 20 nm [sodium citrate concentration of 0.5 mM, Fig. 7(a)] relative to the original peak wavelength of 705 nm. Third, under a more aggressive aggregation condition [a higher sodium citrate concentration of 1 mM, Fig. 7(b)], the differences between PNA probe and PNA-DNA annealing mixtures and between fc, m1, and nc targets are much larger (longitudinal wavelength shift of 10, 20, and 30 nm, respectively), which would allow for a more sensitive DNA detection and a better discrimination between different DNA sequences. Fourth, the possibility of the nc target to bind to the probe sequence through nine complementary bases is affirmed by the retainable AuNRs stability (i.e., comparable peak intensity) relative to the fc and m1 target mixtures. Since the PNA probe has a higher affinity than its DNA counterpart, the nine complementary bases in nc target and probe sequence would enable an effective formation of nc target-PNA duplex to provide the AuNRs with a sufficient protection. Finally, PNA probe induced aggregation is characterized by a remarkable redshift of the transverse peak and blueshift of the longitudinal peak, a typical signature of a side-by-side arrangement of the rods in the aggregates. However, in the presence of PNA-DNA complexes, the reduced but detectable aggregation tends to adopt

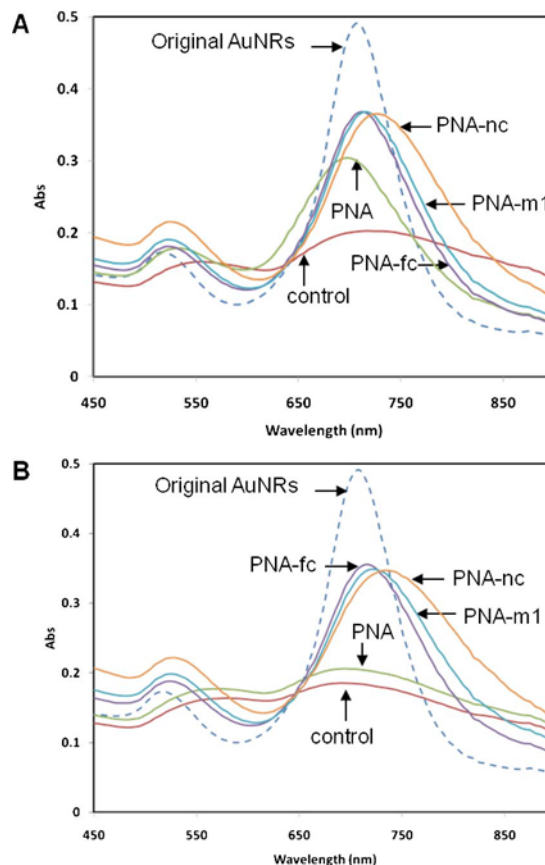


Fig. 7. (Color online) UV-vis extinction spectra of AuNRs (AR 3.0) solutions (dashed lines) and those with the addition of sodium citrate in the absence (bare AuNRs) and presence of single-stranded PNA probe, PNA-DNA complexes with fc, nc, and m1 DNA. DNA concentration is $1 \mu\text{M}$. Sodium citrate concentration is (a) 0.5 mM and (b) 1 mM. All spectra were scanned immediately after the addition of sodium citrate.

an end-by-end arrangement as evidenced by the remarkable redshift of the longitudinal peak and the retainable transverse peak. This observation suggests a potential of using PNA and/or PNA-DNA complexes to assemble nanorods with desirable arrangements.

IV. CONCLUSION

We have discovered an interesting phenomenon that nucleic acid samples of different structures (ssDNA, PNA, dsDNA, and PNA-DNA complex) can bind to CTA⁺-coated AuNRs and retard anionic ion-induced aggregation to different extents. Using this phenomenon, we have developed a UV-vis spectrum assay for detecting specific DNA sequences using ssDNA and PNA as sensing probes. The assay involves no DNA-conjugation and no on-particle hybridization and can display the results immediately upon mixing the annealing solutions with the nanorod solutions. The sensitivity and selectivity of this assay are comparable and better than those using spherical gold nanoparticle-based assays under similar sensing principles (controlled removal of stabilization forces).

ACKNOWLEDGMENT

The authors would like to acknowledge the Agency for Science, Technology and Research (A*STAR), Singapore for the financial support under Grant No. CCOG01_005_2008.

- ¹W. A. Murray and W. L. Barnes, *Adv. Mater.* **19**, 3771 (2007).
- ²M. E. Stewart, C. R. Anderton, L. B. Thompson, J. Maria, S. K. Gray, J. A. Rogers, and R. G. Nuzzo, *Chem. Rev. (Washington, D.C.)* **108**, 494 (2008).
- ³C. S. Thaxton, D. G. Georganopoulou, and C. A. Mirkin, *Clin. Chim. Acta* **363**, 120 (2006).
- ⁴P. Baptista, E. Pereira, P. Eaton, G. Doria, A. Miranda, I. Gomes, P. Quaresma, and R. Franc, *Anal. Bioanal. Chem.* **391**, 943 (2008).
- ⁵W. A. Zhao, M. A. Brook, and Y. Li, *ChemBioChem* **9**, 2363 (2008).
- ⁶E. Dujardin, L. B. Hsin, C. R. C. Wang, and S. Mann, *Chem. Commun. (Cambridge)* **2001**, 1264.
- ⁷B. F. Pan, L. M. Ao, F. Gao, H. Y. Tian, R. He, and D. X. Cui, *Nanotechnology* **16**, 1776 (2005).
- ⁸C. Wang, Y. Chen, T. Wang, Z. Ma, and Z. Su, *Chem. Mater.* **19**, 5809 (2007).
- ⁹H. Nakashima, K. Furukawa, Y. Kashimura, and K. Torimitsu, *Chem. Commun. (Cambridge)* **2007**, 1080.
- ¹⁰X. Li, J. Qian, and S. He, *Nanotechnology* **19**, 355501 (2008).
- ¹¹P. K. Sudeep, S. S. T. Joseph, and G. K. Thomas, *J. Am. Chem. Soc.* **127**, 6516 (2005).
- ¹²W. He, Z. C. Huang, Y. F. Li, J. P. Xie, R. G. Yang, P. F. Zhou, and J. Wang, *Anal. Chem.* **80**, 8424 (2008).
- ¹³Y. F. Huang, Y. W. Lin, and H. T. Chang, *Langmuir* **23**, 12777 (2007).
- ¹⁴J. Pérez-Juste, J. I. Pastoriza-Santos, L. M. Liz-Marzán, and P. Mulvaney, *Coord. Chem. Rev.* **249**, 1870 (2005).
- ¹⁵N. Varghese, S. R. C. Vivekchand, and C. N. R. Rao, *Chem. Phys. Lett.* **450**, 340 (2008).
- ¹⁶S. J. Zhen, C. Z. Huang, J. Wang, and F. Li, *J. Phys. Chem. C* **113**, 21543 (2009).
- ¹⁷M. Sethi, G. E. Joung, and M. R. Knecht, *Langmuir* **25**, 1572 (2009).
- ¹⁸B. Pan *et al.*, *J. Phys. Chem. C* **111**, 12572 (2007).
- ¹⁹G. Kawamura, Y. Yang, and M. Nogami, *J. Phys. Chem. C* **112**, 10632 (2008).
- ²⁰P. K. Jain, S. Eustis, and M. A. Ei-Sayed, *J. Phys. Chem. B* **110**, 18243 (2006).
- ²¹M. Sethi, G. Joung, and M. R. Knecht, *Langmuir* **25**, 317 (2009).
- ²²X. D. Su and R. Kanjanawarut, *ACS Nano* **3**, 2751 (2009).
- ²³R. Kanjanawarut and X. D. Su, *Anal. Chem.* **81**, 6122 (2009).
- ²⁴H. Li and L. Rothberg, *Proc. Natl. Acad. Sci. U.S.A.* **101**, 14036 (2004).
- ²⁵See EPAPS supplementary material at E-BJI0BN-5-013003 for UV-vis spectra of AuNRs coated with nucleic acids but without adding sodium citrate, sequence analysis of the nc target, and the reproducibility of UV-vis measurement.
- ²⁶K. Sato, K. Hosokawa, and M. Maeda, *J. Am. Chem. Soc.* **125**, 8102 (2003).
- ²⁷P. Weroński, Y. Jiang, and S. Rasmussen, *Biophys. J.* **92**, 3081 (2007).
- ²⁸A. Gourishankar, S. Shukla, K. N. Ganesh, and M. Sastry, *J. Am. Chem. Soc.* **126**, 13186 (2004).